

A COMPARISON OF TOKAMAK BURN CYCLE OPTIONS

David A. Ebst, J. N. Brooks, Y. Cha, K. Evans, Jr., A. M. Hassanein, S. Kim, S. Majumdar, B. Misra, and H. C. Stevens

Argonne National Laboratory, Fusion Power Program
9700 South Cass Avenue, Building 205
Argonne, Illinois 60439 U.S.A.

1. INTRODUCTION

Experimental confirmation of noninductive current drive has spawned a number of suggestions as to how this technique can be used to extend the fusion burn period and improve the reactor prospects of tokamaks. Several distinct burn cycles, which employ various combinations of Ohmic and noninductive current generation, are possible, and we will study their relative costs and benefits for both a commercial reactor as well as an INTOR-class device. We begin with a review of the burn cycle options.

Until recently all tokamaks operated with toroidal current generated by an external transformer (OHC). On this basis a reactor would necessarily be operated in a pulsed, ohmically driven (OH) mode. A host of shortcomings are perceived to result in a power reactor operated in this fashion. These problems derive from thermal fatigue in high temperature components, mechanical fatigue associated with magnetic field fluctuations, and the costs of thermal and electrical energy transfer and storage.

The STARFIRE reactor design^{1,2} was the first analysis of a tokamak operating in a purely noninductive burn mode with continuous wave (CW) injection at the lower hybrid frequency. The principal concern with CW operation is the efficiency of generating the toroidal current. Figure 1 illustrates the typical power, P_d , required to drive current in a CW tokamak the size of STARFIRE, assuming moderate beta, low safety factor ($q = 1.0-2.5$) and various efficiencies $\gamma \equiv I_0 (R_0/7.0 \text{ m})(n/10^{20} \text{ m}^{-3})/P_d$ for high-speed current drive (energy added to suprathermal electrons); we define I_0 to be toroidal current, R_0 is major radius, n is the average electron density, and units are SI and KeV. This class of drivers includes the lower hybrid (slow), magnetosonic (fast), and electron cyclotron wave. In the best theoretical case (relativistic limit) $\gamma = 0.2$ A/W, whereas present-day experiments^{3,4} report $\gamma = 0.017$. From the figure we see driver power is minimized by operating at $T_e > 12$ keV; there is also great incentive to achieve $\gamma > 0.1$ since driver power in excess of 200 MW will be an expensive item if driver cost exceeds $\sim \$1/W$. The net electric power is plotted from the approximate formula $P_{\text{net}} = 0.357 P_{\text{th}} - 73 \text{ MW} - (P_d/0.7)$, where the thermal power is due to

DISCLAIMER

This report was prepared as an account of work sponsored by an agency of the United States Government. Neither the United States Government nor any agency thereof, nor any of their employees, makes any warranty, express or implied, or assumes any legal liability or responsibility for the accuracy, completeness, or usefulness of any information, apparatus, product, or process disclosed, or represents that its use would not infringe privately owned rights. Reference herein to any specific commercial product, process, or service by trade name, trademark, manufacturer, or otherwise does not necessarily constitute or imply its endorsement, recommendation, or favoring by the United States Government or any agency thereof. The views and opinions of authors expressed herein do not necessarily state or reflect those of the United States Government or any agency thereof.

MASTER

alpha heating, the absorbed driver power, and neutron heating with blanket enhancement: $P_{th} = P_{\alpha} + P_d + 1.14 P_n$. Also we note P_{net} maximizes at $T > 12$ keV; $\gamma > 0.06$ A/W may suffice to achieve acceptable net power. The penalty for operation above ~ 12 keV is the rapid increase of E_M above 11 T. The credibility and reliability of such very high field TF magnets is called to question.

In the event that γ cannot be increased we could consider a pulsed operating mode in which the noninductive driver is used only during low density periods, when the ratio I_0/E_d is large. One possibility here is to use noninductive current drive during such periods of low density operation, driving the current above the minimum value needed for fusion operation, and then permitting the current, I , to decay resistively during a brief period of high density fusion operation until the cycle must be repeated. This mode,⁵⁻⁷ called internal transformer (IT) operation, completely eliminates the external transformer but requires oscillating fusion power and equilibrium field coil (EFC) magnetic fields.

Of more practical interest is a hybrid mode^{5,9} in which I remains constant, driven at high density during the fusion burn by an external transformer, and at low density by a noninductive driver while the transformer is reset. This cycle, shown schematically in Fig. 2, still has fusion power oscillations and vertical field fluctuations associated with the low density transients.

At the conclusion of our work we will argue that pure CW operation is the only cycle which is clearly superior for a commercial reactor, whereas the hybrid mode could be a worthy goal for a smaller INTOR sized tokamak if current drive efficiency, γ , does not improve beyond the values currently demonstrated. These results are based on comparative studies of the reactor subsystems which are affected by burn cycle details. Our models for these subsystems are presented in Section 2. Density and temperature transients present varying heat loads to the first wall, limiter/divertor plates, and blanket structures and may also trigger major disruptions which can damage the plasma-side materials. These thermal effects, which mostly shorten lifetime and reduce the reactor's availability, are discussed in Section 3. Other effects of cyclic operation, which are analyzed in Section 4, result in capital cost differences among the various burn cycle options. Examples of these problem areas are mechanical fatigue in magnets and support structures, eddy current heating in magnets, electric power supply and thermal energy storage costs, and costs of the current drive system. In Section 5 we compare the cost and performance of commercial reactors designed for the various burn cycles, and in Section 6 we do the same for a smaller device like INTOR.

2. SUBSYSTEM MODELS AND DESIGN OPTIONS

Those commercial reactors which employ noninductive drivers have a major radius $R_0 = 7.0$ m, and the reactor with the OH cycle has $R_0 = 8.0$ m in order to achieve burn periods $t_f \geq 10^3$ s. Both designs perform similarly to STARFIRE with fusion power $P_f = 4000$ MW and a neutron wall load $W_n = 4$ MW/m². Our INTOR analysis is based partly on the ANL design of a DEMO reactor.⁹ We consider multiple concepts for most subsystems in order to reflect the uncertainty of future technology. The choices will be briefly enumerated here; a more detailed account of our analysis is available in Ref. 10-12.

For the limiter (or divertor plate) structure we have studied two basic alternatives. One system, representative of near-term technology, has a copper alloy for the heat sink structure and is water cooled (4 MPa, 130°C). A more advanced alternative has a vanadium alloy heat sink

with liquid lithium coolant (4 MPa, 210°C). The front face of the limiter (that portion closest to the plasma) is modeled as a flat slab with a variable thermal load, $W_{FF} = 1.5-3.5 \text{ MW/m}^2$, and the leading edge is analyzed as a cylinder with thermal loads of $W_{LE} = 0.75-1.75 \text{ MW/m}^2$. We assume the entire limiter is laminated with a surface material (tiles) specifically designed to reduce sputtering. At the front face we pick beryllium as a typical coating, while near the leading edge a larger number of options are possible, and we consider both beryllium and tungsten as coatings.

The first wall is treated as a simple bank of cooling tubes. One option is water cooled (15 MPa, 300°C) with prime candidate alloy (PCA) for the tube structure. We use 20% cold worked 316 stainless steel to model the PCA properties. At these high pressures a thin wall tube requires a small inner radius, and we consider $r_i = 3-10 \text{ mm}$. The more advanced design utilizes liquid lithium (2 MPa, 350°C) as a coolant and vanadium as the structure. The low pressure permits relatively large radius piping; $r_i = 25 \text{ cm}$ is chosen. The surface heat load $W_{FW} = 0.5-1.0 \text{ MW/m}^2$, is due mainly to photon radiation, so the first wall is taken to be bare structure.

Radiation damage is estimated by choosing a correlation between the neutron wall load and the thermal loads: $W_{FW} = 0.25 W_n$, $W_{LE} = 0.4 W_n$, and $W_{FF} = 0.8 W_n$. Based on a survey of materials properties we assign the following neutron radiation limits to structural materials: Cu, 4 MW-y/m^2 ; PCA, 12 MW-y/m^2 ; and V, 24 MW-y/m^2 . Likewise we limit the maximum temperatures as: Be, 700°C; W and V, 600°C; PCA, 500°C; and Cu, 250°C.

Commercial reactors with pulsed fusion power require thermal storage during the dwell period to supply steady electrical power to the utility's grid. We have calculated the cost of thermal storage for two attractive options. The near-term system employs high pressure water and steam, and a more advanced system, which could be more economical, uses liquid metals to store energy.

Electric power supplies are needed to transfer energy to magnets. The EF coils are powered through a silicon controlled rectifier (SCR) assembly from a motor-generator-flywheel (MGF) set. A similar power train is used to reset the OH coil between fusion burns of the ohmically driven and hybrid burn cycles. A third power system is needed for the ohmic burn cycle in order to supply high loop voltage for startup; this power supply dumps considerable energy from the OHC through a resistor.

The pulsed superconducting magnets (the OHC and EFC) as well as the TF coils utilize the multifilament cable described in the STARFIRE design.¹ Only niobium-titanium was considered for the OHC since the pulsed nature of its operation would make Nb_3Sn a poor alternative.

The toroidal field coil (TFC) model is a critical input to this study since the TFC is a very expensive system and is sensitive to fatigue from out-of-plane bending. Our focus is on one particular TFC design.¹ The superconductor is housed in a helium vessel at 4.2 K which is suspended by thin struts (of low thermal conductivity) from an enclosing room temperature vacuum tank. Both vessels are constructed from Type 316 LN stainless steel (annealed). The overturning moments on the TFC are resisted by the steel support cylinder (inboard) and shear panels (outboard). This leaves unsupported free spans, along the top and bottom legs of each TFC, which are restrained from gross bending by the stiffness of the vacuum tank. The superconducting cable is coated by two

algorithms. A near term estimate, based on current material costs and fabrication techniques, is

$$C_I = (m_{Cu} \times \$160) + (m_{NbTi} \times \$460) + (M_{st} \times \$30) ,$$

where m_i is the mass in kg of the cable material (copper, superconductor, and steel). However, if tokamak reactors are commercialized we would expect significant price reductions due to mass production and learning experience. Future technology might provide¹ a cost

$$C_{II} = (m_{Cu} \times \$34) + (m_{NbTi} \times \$120) + (m_{ss} \times \$17) + (m_{NbSn} \times \$230) ,$$

where an advanced superconducting alloy is included. We compute the steel vacuum tank cost based on \$24/kg.

All magnets are designed with adequate steel structure to survive the life of the power plant. The total number of fusion cycles in the reactor lifetime is based on a 40-y assumed lifetime and 80% availability (1.0×10^9 s of operation). Our philosophy is that all burn cycles must achieve this high availability to be of interest to a utility. We attempt to calculate burn cycle requirements and system capital costs needed to approach these goals. All costs are in 1983 dollars. An accurate estimate of subsystem reliability, mean time to replace failed components, and system availability is obviously not possible at present. However, the data presented here provide a useful comparison of the relative attractiveness of the various burn cycles.

3. THERMAL EFFECTS OF CYCLIC OPERATION — FATIGUE AND DISRUPTIONS

Our aim is to maximize first wall and limiter lifetime against simultaneous failure modes. First, thermal fatigue is calculated, and we find that cycle life generally decreases for thicker structures and coatings. Next we study material loss from disruptions and show how component cycle life increases with thicker structures and coatings. The component dimension corresponding to the intersection of these life curves is considered optimum for obtaining the longest cyclic life. Then the minimum fusion burn length is found such that the total cyclic life is not shorter than the expected component life against radiation damage.

We illustrate our lifetime analyses by reference to Fig. 3. The thermal stress fatigue cycle lifetime, N_f , for first wall PCA is displayed for three different heat loads. As the tube wall gets thicker (δ increasing) thermal stress increases and N_f decreases dramatically. Likewise, increases in W_{FW} also severely reduce the fatigue life. We note a lower limit to δ , due to primary stress from the coolant, is set by permitting an upper tolerance of 5% radiation-induced creep strain at the end of the tube life. The upper limit to δ is reached when the plasma side (outside) of the tube begins to exceed 500°C; above this temperature the structural qualities of PCA deteriorate. The significant factor to us is that thicker tubes will withstand more damage from major disruptions. Two curves in the figure show the number of fusion cycles of operation before disruptions perforate a tube (assuming 70 μ m of erosion at the same spot each time) if the average frequency of disruptions is one out of a thousand ($f=10^{-3}$) or one out of ten thousand ($f=10^{-4}$) burn periods. For a given probability of disruptions, f , and a given wall load, W_{FW} , there is an optimum thickness which gives the longest cyclic lifetime against both thermal fatigue and disruptions. Now, for the maximum N_f corresponding to the optimum δ we would desire a tokamak burn period, t_b , sufficiently long that fatigue and disruptions are not more limiting than radiation damage. This minimum burn length is $t_b = (L_{rad}/W_n N_f) - 100$ s, where we allow 100 s between burns. L_{rad} is the

fore shorter in-reactor life. In the second place these higher thermal loads exacerbate the fatigue problem and generally require longer burns in order to not surpass the limit on cycle lifetime.

Finally, we caution that our results only display general trends. Reactor availability should improve with several factors: use of more radiation and fatigue resistant materials; reduction in the frequency and severity of disruptions; reduction in net sputtering erosion; selection of disruption resistant materials; operation at lower wall loads; as well as operation with longer fusion burns.

4. CAPITAL COSTS OF CYCLIC OPERATION

One obvious penalty for the OH and hybrid burn cycles is the large and expensive OHC (transformer). The base price for a commercial reactor varies from \$30M to \$80M (C_{11} and C_1 , respectively) if fatigue is not a factor. However, for lifetime stress cycles $N_f \geq 3 \times 10^4$ additional steel is needed in the winding pack so the stress is reduced adequately to eliminate failure due to mechanical fatigue. For $N_f \geq 10^6$ this increases the OHC cost by $\geq 20\%$ and also reduces the volt-seconds stored in the OHC. Figure 6 indicates these variations with N_f for INTOR.

With regard to the EFC system, we note that the OH and hybrid cycles require an OHC in the hole in the doughnut, and this transformer impedes the design of optimally located EF coils. For a commercial reactor we find the EFC stored energy increases $\geq 10\%$ (5.6 GJ to 6.3 GJ) when the EFC is constrained by the OHC location. This translates, of course, into a more expensive EFC system. As with the OHC we must increase the structure fraction of the winding to accommodate fatigue as the cyclic lifetime increases. Increasing N_f from $\sim 10^4$ to $\sim 10^6$ will increase the cost of the EFC system by fifty per cent. Figure 7 displays this result for INTOR, assuming the OH cycle is employed. If the hybrid mode is utilized the vertical field variations are smaller (due to only the β_p fluctuations during the dwell phase) so the stress variations are smaller and less structure is required to withstand fatigue.¹²

The burn cycle effects on the TFC are mainly associated with the varying out-of-plane bending forces which accompany the vertical field oscillations. A fracture mechanics analysis of the unsupported spans of the TFC and the intercoil shear panel was performed and the structural thickness was inferred which would promise fail-safe operation for the reactor lifetime. We assumed starter cracks to be 10% of the member's thickness. The resulting cost variation is shown in Fig. 8 for a commercial reactor. As expected, the cost is level up to $N_f \sim 10^4$. Hence, a reactor with a day-long burn ($t_f \sim 10^5$ s) has TFC structure no more expensive than that for a CW reactor ($t_f \sim 3$ mo., $N_f \sim 200$). However, shorter burns accumulate fatigue damage very quickly. For short burns ($t_f \sim 10^3$ s, $N_f \sim 10^6$) the incremental structural costs become prohibitive. We caution, though, that our cost estimates may be too high at large N_f . At tank costs of \$100M to \$200M the steel side walls are in the range of 20-cm to 30-cm thickness. It may prove impractical to form such large, thick members. The prohibitive costs at this point would drive us to consider alternative structural support.

We note that there are large differences among the burn cycles for a fixed N_f . The double-swing OH cycle (in which the toroidal plasma current is reversed in direction each cycle) has the largest stress fluctuations and hence requires the most massive structural support. For the same N_f a single swing OH cycle results in cost savings. Even more attractive is the hybrid burn cycle, since the stress fluctuation is so modest ($R_0 = 0.5$). For IT operation the relatively small stress fluctuations are overshadowed by the much larger number of pulses envisioned for

radiation lifetime ($12 \text{ MW}\cdot\text{y}/\text{m}^2$ for PCA). These minimum values for t_f are given in Fig. 4 by the dashed curves, and the lower abscissas provide the first wall replacement period at 80% availability [$T = L_{\text{rad}}/W_n/0.8$].

An examination of Fig. 4 can be revealing. For example, the influence of disruptions on desired burn length can be nonlinear. A reduction of the thermal energy dump by a factor of two ($700 \text{ J}/\text{cm}^2$ to $380 \text{ J}/\text{cm}^2$) results in a reduction of t_f by a factor of five. In fact, there is a threshold energy density which results in erosion. Below $300 \text{ J}/\text{cm}^2$ no PCA is melted or vaporized; in this case very thin wall coolant tubes would be desired, large N_f would result, and t_f could be just a few minutes. On the other hand, t_f is proportional to the probability of having a disruption. If as many as 1% of the shots terminated with disruptions then t_f would have to exceed 10 h even for moderate damage ($70 \mu\text{m}$ lost each time).

PCA represents a first wall structure based on near term materials, as might be used in INTOR. Figure 4 shows that radiation damage limits the life of PCA to $T_{\text{PCA}} = 4\text{-}7$ calendar years at reactor wall loads of $W_n = 2\text{-}4 \text{ MW}/\text{m}^2$. Vanadium alloys, with superior radiation resistance, promise lifetimes roughly twice as long as PCA and represent a desirable goal for reactor R&D. With vanadium, thermal fatigue is much less of a problem than with PCA, and coolant tubes can be much thicker than the PCA first wall. In fact, the temperature limit of 600°C acts to constrain the tube wall to $\delta \leq 10 \text{ mm}$, and erosion from disruptions dominates the calculation of cyclic lifetime for V. As seen in the figure, t_f must be roughly as long for both PCA and V structure. In the worst case depicted, with severe disruptions, $t_f \geq 8 \text{ h}$ may be necessary to guarantee first wall survival.

A similar analysis of the limiter's front face and leading edge was performed. In this case thermal fatigue is a concern for the substrate heat sink, which is a structural member, and not for the coating, which will still function even if weakened by cracks. However, erosion from disruptions affects the coating, which must not be permitted to wear through and expose the bare substrate to the plasma. The burn goals for the front face of the limiter with a Be coating are shown in Fig. 5. We see relatively short t_f ($\leq 1 \text{ h}$) may suffice to achieve the radiation limited life of a heat sink, like Cu, which has poor radiation resistance. In order to achieve the benefits of advanced materials like V the burn period must exceed several hours if the disruption probability is $f > 10^{-3}$. Results for the leading edge are similar, except that if the plasma temperature is so low ($\leq 30 \text{ eV}$) that sputtering is negligible then W makes an ideal coating. Tungsten is almost immune to disruption damage, so a thin coating ($\leq 1 \text{ mm}$) would provide protection, and we find under these circumstances both Cu and V substrates have very large cycle lifetimes. In this special case t_f could be quite small (a few minutes).

We conclude this section with some general observations. Our results typically show that "near-term" structures such as copper limiters and a steel first wall can tolerate relatively short fusion burns because their radiation life is thought to be short. In order to take full advantage of advanced materials with longer radiation life it will be necessary to arrange for longer burns (CW or long pulse operation). On the other hand, reactors with short burns ($t_f \sim 100 \text{ s}$), operating in the internal transformer mode, will not be attractive unless disruption frequency is $f \leq 10^{-5}$ and sputtering erosion is $\delta \leq 1 \text{ cm}/\text{y}$.

Generally speaking, the higher thermal loads are more demanding on our designs. In the first place this is because we have assumed the higher thermal loads are associated with higher neutron damage and there-

the life of the reactor ($N_f \geq 10^6$), with the net result that this cycle is likely to be the least attractive in terms of TFC structural costs.

We see that a double swing OH cycle operating with a one-hour burn ($N_f \sim 3 \times 10^5$) will entail capital costs at least \$100M higher than a reactor operating in the CW mode. This disparity is greatly reduced if the ohmic burn period can be extended to 8 h or more. If neither of these options is available but a hybrid burn cycle is used, then any fusion cycle period exceeding about 30 min becomes competitive. The internal transformer cycle seems unattractive since it has such a tremendously large total number of cycles in the reactor lifetime ($N_f \geq 10^6$).

Pulsed operation also adds eddy current heating to the superconducting magnets, which increases the electric power and cost of the cryogenic system. The heat production varies as $B^2 = t_{EP}^{-2}$, where t_{EP} is the period of vertical field swing, and the average refrigerator power $\propto \tau^{-1}$ where τ is the total burn cycle period available to remove the extra heat from the coils. For a commercial reactor τ presumably is so long ($\geq 10^3$ s) for the OH burn cycle that a switch from OH to hybrid or CW operation does not significantly benefit the reactor on account of eddy current heating. However, for INTOR the OH burn is quite short (~ 100 - 200 s), and a design for the hybrid burn cycle would extend τ to $\geq 10^3$ s as well as increase t_{EP} , so we would expect a substantial savings ($\sim \$10M$) by electing the hybrid burn cycle for INTOR.

With regard to energy storage and transfer systems we find the important concern is the down time between fusion burns, rather than the length of the burn. There is an optimum sequence and time for events during this transient phase which will minimize the costs of the hardware involved.

Consider first the optimization for commercial reactors, which require thermal energy storage during the dwell. A 4000 MW thermal reactor must store hundreds of gigajoules for reasonable dwell periods, and, at a typical storage cost of \$2M-\$4M per second,^{10,12} this motivates the desire for short dwell periods. However, short dwells increase the cost of EFC power supplies and, for the OH and hybrid cycles, of the OHC power supplies, since these magnets must be energized on a shorter time scale. Likewise, for the hybrid and IT burn cycles, the noninductive current drive power supplies become more costly for shorter dwells, since the reversed emf in the plasma becomes larger. Details of the analysis are given in Ref. 12, and we present here only the relevant conclusions.

For the commercial reactor operating in the double-swing OH mode we find the optimum dwell period is $t_{dw} = 25$ s (to reset the transformer), $t_{OH} = 10$ s (to initiate and later ramp down the current), and $t_{EP} = 10$ s (to reach ignition and later reduce the plasma pressure), with a total $t_{down} = 55$ s. Including a high pressure water storage system for thermal energy and the requisite power supplies for the OHC and EFC we find the minimum cost for these systems is $\sim \$430M$, a very large capital investment for an ohmically operated reactor. Use of more advanced technology (liquid metal thermal storage) may reduce this cost to \$309M, which is a substantial savings.

For the reactor operating in the hybrid mode an additional option appears, namely the size of the OHC. Since the external transformer need not supply startup volt seconds it may be smaller and still provide the same t_f as achieved by the OH burn cycle. We find a maximum field of 6.5 T in the OHC provides the same burn length as a 10.0 T OHC for the conventional OH-driven reactor. For this particular hybrid cycle we find

the optimum transient phase has $t_{dw} = 45$ s and $t_{EP} = 13$ s with water thermal storage, noninductive driver cost of \$1.50 per watt injected into the plasma, and assuming the already demonstrated $\gamma = 0.017$ A/W. The associated minimum cost for these systems (excluding auxiliary power, ~75 MW, assumed needed for ignition) is \$371M, which is roughly \$60M less than the costs for the OH driven reactor. For liquid metal storage the total cost is even lower, \$256M. Interestingly, we find that further increases in γ will not benefit hybrid operation since at low density the driver power is already small enough that it does not figure prominently in the total cost of power supplies and energy handling.

The cost tradeoffs for INTOR operating in the hybrid mode are seen in Fig. 9. INTOR has no need for thermal storage so the poloidal field power supplies and current drive system alone determine the optimum transient phase. Here $2t_{EP} + t_{dw} = t_{down} = 340$ s, in order to retain a duty factor goal of 83% (since $t_f = 1700$ s in the hybrid mode). Costs are minimized by lengthening the transient period, so there is no motivation to reset the transformer rapidly. This is because energy is taken from the grid, rather than from a motor-generator-flywheel; for INTOR the power supply costs are more significant than the electric energy cost. We find the best case has $t_{dw} = 200$ s and $t_{EP} = 70$ s. The total costs are reduced by increasing plasma resistance, R_p , as the OHC is reset. We also find our minimum cost is relatively insensitive to the current driver cost and to γ , since the density n_{20} may be made very low during the dwell period.

With respect to thermal storage and power supplies we find the IT cycle is always more expensive than the hybrid mode of operation and will likely result in substantially more fusion burns. The best mode of operation from this viewpoint is CW. Excluding power supplies for auxiliary heating and current drive, a CW commercial reactor needs only ~\$10M of power supplies, for the EFC. This is due to elimination of the OHC power supplies and the thermal storage plant. The final choice among burn cycles requires a consistent comparison of all costs, however, and this will be given in the next section.

5. BURN CYCLE COMPARISON FOR COMMERCIAL REACTORS

For the conventional OH cycle, first wall and limiter fatigue lessens and capital costs decrease as the burn period, t_f , lengthens, as shown in Fig. 10. The solid symbols on the upper abscissa are goals for t_f which are needed to reduce cyclic life limitations for "worst case" disruptions (e.g., $f = 10^{-3}$, 800 J/cm²). We see that day-long burns are needed to achieve these goals and also to minimize capital costs. However, $t_f \geq 10^4$ s may be unlikely for an 8-m tokamak unless the resistivity can be reduced below the classical Spitzer value. Even in the long t_f limit the direct capital costs of the fusion power plant exceed the (CW) STARFIRE cost by a large fraction (cost is normalized to the STARFIRE direct capital cost¹). With advances in technology (liquid metal thermal storage and reductions in costs of magnet fabrication, C₁I) the cost will still exceed the STARFIRE cost by 20%.

Of course, the STARFIRE study was predicated on the achievement of efficient current drive, $\gamma = 0.14$ A/W, and, if the best γ should in practice be smaller, this may adversely affect the economics of the CW burn cycle. Figure 11 suggests that the goal for current drive research is $\gamma \geq 0.07$ A/W in order to have a reasonable net power production. Thus, roughly a four-fold improvement in γ is needed over the current experimental results.^{3,4} A breakthrough in driver technology could relax this γ requirement somewhat; for example, $\gamma \geq 0.04$ A/W is probably acceptable if the driver efficiency $\eta_d = 0.70$. Driver cost reductions (below \$1/W)

apparently are not as important for a CW reactor as are improvements in η_d (above 0.50).

The IT cycle cost was parameterized in terms of the length of the burn period (which increases by using a larger overdrive and current boost, $\Delta I/I_0$, during the dwell), and total costs minimized at $\Delta I/I_0 = 1.2$. However, capital costs were still ~25% more than the CW STARFIRE cost, regardless of the ratio γ/n_{20} . Moreover, the IT cycle will likely result in an order of magnitude more burn cycles, $N_f = 10^6$, than the OH mode of operation. This is clearly undesirable when thermal fatigue and disruptions are expected to limit the first wall and limiter lifetime and the reactor's availability.

For small but achievable values of γ we find the hybrid cycle is always more attractive than the OH and IT operating modes. We display the cost variations with the OHC flux in Fig. 12, assuming advanced thermal storage and coil fabrication techniques. A comparison of these curves with Fig. 10 indicates that hybrid operation is less expensive provided $\gamma/n_{20} \geq 0.5$. For a burn of $t_f = 8000$ s (assuming $R = R_{sp}$) the OH driven reactor costs 37% more than STARFIRE ("L1" curve, double swing) whereas the hybrid reactor costs 15%-18% more than STARFIRE. The cheapest hybrid reactor ($t_f = 4000$ s) costs only ~10% more than STARFIRE. Among the pulsed burn cycles the hybrid operating mode clearly promises the lowest direct capital cost; however, CW operation of a commercial reactor requires a negligible number of burn cycles, which augurs for the longest lived plasma chamber and the highest reactor availability. In the best case, the CW reactor may also be 10% less expensive than any pulsed reactor.

Based on our burn cycle study for commercial reactors we can make several conclusions, which fall into various categories. In the area of operating goals and material properties we find:

- Double-swing OH operation results in cost savings compared to single swing OH operation.
- For either OH burn cycle we find reactor cost minimizes at fairly long burn times, $t_f \geq 10$ -20 h.
- For any cycle with a fusion period as short as ~1 h there is a first wall limiter life limit imposed by thermal fatigue, especially if there are frequent or severe disruptions. Thermal fatigue ceases to be a major concern if disruptions are very rare ($f < 10^{-4}$) or of low energy density (≤ 200 J/cm²), if vapor shielding is significant, or if the melt layer is not lost from the affected surface. On the other hand, a single disruption could be fatal if it initiates cracks in the first wall which lead to premature thermal failure.
- Use of materials with superior thermal fatigue resistance may permit shorter fusion burns for a given replacement period of the reactor component. However, if structural materials such as vanadium are selected for their high radiation resistance, then there appears to be a need to extend burn lengths in order that cyclic effects not prevent the achievement of longer in-reactor life. Considering the uncertainties surrounding disruption-induced damage, the full benefits of radiation resistant materials can probably only be guaranteed with the CW burn cycle.

Regarding issues of plasma physics we can reach several conclusions:

- If very low plasma edge temperatures (< 50 eV) are possible then tungsten could serve as an ideal thin limiter leading edge coating with the result that disruptions and thermal fatigue would have negligible impact on the leading edge lifetime.
- Our understanding of what initiates disruptions must improve. If disruptions are eliminated by merely holding the toroidal current constant, then the IT and hybrid cycles can be attractive compared to the OH cycle. However, if density variations can also trigger disruptions then the CW cycle may be the only good alternative.
- Lower current (higher beta) equilibria are beneficial to tokamak reactors, allowing longer burns for inductive current drive, due to the lower loop voltage, and permitting smaller driver power for noninductive current drive.
- We can achieve longer inductive burn periods if means are found to substantially lower plasma resistivity, e.g., by lower Z_{eff} , eliminating trapped electrons, or modifying the electron distribution function.
- On the other hand, the conventional OH cycle appears virtually obsolete since, even for present-day experimental results ($\gamma/n_{20} \approx 0.5$), we find noninductive current drive efficiency is adequate to make the hybrid cycle result in a cheaper reactor. Likewise, for reasonable t_f (≥ 20 min) the hybrid cycle is better than the IT cycle.
- If noninductive current drive can achieve $\gamma \geq 0.07$ A/W then CW operation is by far the best choice. We should aggressively seek improvements or alternatives (fast wave, low frequency compressional Alfvén wave¹³) to the lower hybrid wave for noninductive current drive.

In the area of the driver technology we conclude:

- Reductions in driver system cost (to $< \$1/W$) are always desirable, and we note that lower frequency ($\sim 1-100$ MHz) drivers come closest to this goal. However, the OH reactor cycle costs $\sim 20-25\%$ more than STARFIRE, so we infer that an equivalent sum ($\sim \$400-500M$) can be spent on a current driver system before the CW reactor would become more expensive than the OH reactor.
- Of greater significance than cost is the overall power efficiency of the current drive system. Drivers projected to have low η_d (e.g., ECRH) need higher γ to achieve acceptable net reactor power with CW operation.

6. BURN CYCLE COMPARISON FOR INTOR

INTOR contrasts with a commercial tokamak by being a minimum-size device with a small hole-in-the-doughnut. Thus it provides barely enough OHC flux to provide any length of a plasma burn. Based on the INTOR parameters of Ref. 14 we might expect $t_f \approx t_r \approx 200$ s for operation in the OH mode, resulting in a duty factor $f_D = 0.81$, if the down period is $2t_{\text{EF}} + 2t_{\text{OH}} + t_{\text{dw}} = 46$ s. Assuming 1×10^5 low-power shots are followed by operation to achieve a fluence of 5.0 MW-y/m² this would result in a cyclic lifetime $N_f = 7.0 \times 10^5$. We optimized the DEMO design,⁹ which is similar to INTOR, for the hybrid mode, which yields $t_f = 1550$ s, keeping the duty factor fixed at 0.81. The resulting design only requires $N_f = 1.8 \times 10^5$ to achieve the same fluence goals, so substantial reduction in

lifetime cycles is possible in this mode.

The cost savings due to less mechanical fatigue in the magnets is large, as shown in Table 1. Likewise, the extended down period reduces power supply costs. The required current driver cost is a small penalty since, under these circumstances, the driver power is quite modest, ~16 MW. Thus, with such a long period to reset the OHC, we find that the capital cost is insensitive to the exact value of γ or to the cost of the driver (in the range \$1-2/W).

The direct capital costs of the DEMO, operating in the OH mode, were compared with Case 8 of the INTOR design¹⁴ which is rf heated; see Table 1. For the variable cost accounts which are sensitive to the burn cycle option we get a total of \$559M for the DEMO model, compared to \$566M for Case 8. (Agreement is somewhat fortuitous as DEMO has a larger TFC bore which inflates its cost, but a smaller, cheaper EFC, since it has no poloidal divertor.) In contrast, designed for the hybrid cycle the DEMO model would cost only \$369M for these cost accounts. Including fixed cost accounts, we find the hybrid cycle would total \$883M direct capital cost compared to \$1073M for the OH cycle DEMO or \$1080M for the INTOR Case 8. The \$190M savings represents an ~18% reduction in direct capital cost in INTOR by adopting the hybrid burn cycle. This is a substantial savings.

7. EPILOGUE

It is difficult to make sweeping judgments of the relative merits of tokamak burn cycles because a power reactor is such a complex machine with so many operating variables. Yet, in addition to the general trends we have explored, we can point to two other aspects of this problem which are hard to quantify but may be pivotal to the commercial success of tokamaks. First, noninductive current generation may provide an opportunity to tailor the current density profile in order to achieve very stable equilibria. This extra flexibility may not be so easily achieved inductively, and thus CW operation may permit operation at higher β than the OH burn cycle. Finally, the very complexity of a tokamak reactor is a tremendous incentive to achieve CW operation. At this early stage we cannot possibly estimate the reliability of millions of components, pumps, valves, motors, etc., when operating through repeated transients. Reliability and, hence, availability is doubtless far easier to achieve with CW operation, and this will weigh heavily in the final choice among burn cycles.

REFERENCES

1. C. C. Baker et al., "STARFIRE - A Commercial Tokamak Power Plant Study," Argonne National Laboratory Report, ANL/EPP/80-1 (1980).
2. D. A. Eist et al., *J. Fusion Energy* 2 (1982) 83.
3. V. Porkolab et al., "Lower Hybrid Current Drive and Heating Experiments at the 1-MW RF Power Level on Alcator C," 11th European Conference on Controlled Fusion and Plasma Physics, Aachen, West Germany, 1983.
4. R. Motley et al., in Proc. of IAEA Technical Committee Meeting, Culham, England, CLM-CD (1983), Vol. 11 (1983), 299.
5. N. J. Fisch, "Operating Tokamaks with Steady-State Toroidal Current," Princeton Plasma Physics Laboratory Report, PPPL-1772 (1981).
6. N. J. Fisch, in Proc. 3rd Joint Varenna-Grenoble International

Symposium on Heating in Toroidal Plasmas, EUR7979EN, Vol. 111 (1982) 841.

7. C. E. Singer and D. R. Mikkelsen, J. Fusion Energy 3 (1983) 13.
8. R. A. Bolton et al., in Proc. 3rd Top. Mtg. on Technology of Controlled Nuclear Fusion, CONF-780508, Vol. 11 (1978) 824.
9. M. A. Abdou et al., "A Demonstration Tokamak Power Plant Study (DEMO)," Argonne National Laboratory Report, ANL/FPP-82-1 (1982).
10. D. A. Ehat et al., "Tokamak Burn Cycle Study," Argonne National Laboratory Report, ANL/FPP/TM-178 (1983).
11. D. A. Ehat et al., "A Comparison of Pulsed & Steady State Tokamak Reactor Burn Cycles-Part I: Thermal Effects and Lifetime Limitations," Nucl. Eng. and Design/Fusion (to be published, Vol. 2, Issue No. 4, 1985).
12. D. A. Ehat et al., "A Comparison of Pulsed and Steady State Tokamak Reactor Burn Cycles-Part II: Magnet Fatigue, Power Supplies and Cost Analysis," Nucl. Eng. and Design/Fusion (to be published, Vol. 2, Issue No. 4, 1985).
13. D. A. Ehat, J. Fusion Energy 1(1981) 357.
14. W. M. Stacey, Jr. et al., USA FED-INTOR/82-1 (1982).

Table 1. Reference Burn Cycles and Direct Capital Cost for Model Factor (\$M, 1983)

Item	Variable	Single Swing OH Cycle	Hybrid Cycle	
Fusion burn	t_f (s)	200	1350	
EFC ramp	t_{EF} (s)	10	50	
OH high-power ramp	t_{OH} (s)	5	0	
Dwell (reset OHC)	t_{dw} (s)	16	257	
Cycle period	$\tau = t_f + 2 t_{EF} + 2 t_{OH} + t_{dw}$	246	1907	
Duty factor	$f_D = t_f/\tau$	0.813	0.813	
Fluence	Φ (MW-y/m ²)	5.0	5.0	
Full power wall load	W_n (MW/m ²)	1.3	1.3	
Total burns	$N_f = 1 \times 10^5 \times \frac{\Phi}{W_n \tau}$	7×10^5	1.8×10^5	
Ignition power/duration	P_{ICRH} (MW)/ t_{ICRH} (s)	50/10	50/10	
RFCD power/duration	P_{RFCD} (MW)/ t_{dw} (s)	0/0	18/257	
OHC/dump resistor power	P_{OH} (GW)	1.35	0	
MCF stored energy	U_{MCF} (GJ)	10.5	10.5	
OHC reset power	P_{OH}^* (GW)	0.422	0.042	
EFC ramp power	P_{EF} (GW)	1.132	0.113	
Current drive at low density	γ/n_0^2 (A/W)	---	1.0	
Resistance during dwell	R^* (n Ω)	---	25	
			<u>INTOR</u>	
TFC, including structure	C_{TFC} (\$M)	220	(174 ^a)	153
OHC + EFC	$C_{OHC} + C_{EFC}$ (\$M)	80	(138 ^b)	67
OHC dump resistor/switch	C_{OHPS} (\$M)	22	} (172)	0
SCR + MCF	$C_{SCR} + C_{MCF}$ (\$M)	144		42
ICRH for ignition	C_{ICRH} (\$M)	79	(82)	79
RFCD during dwell	C_{RFCD} (\$M)	0	(0)	27
Cryogenics for eddy heating	C_{cryo} (\$M)	14	(n.a.)	1
TOTAL COST (\$M)		559	(566)	369

^aINTOR has smaller TFC bore.

^bINTOR has poloidal divertor.

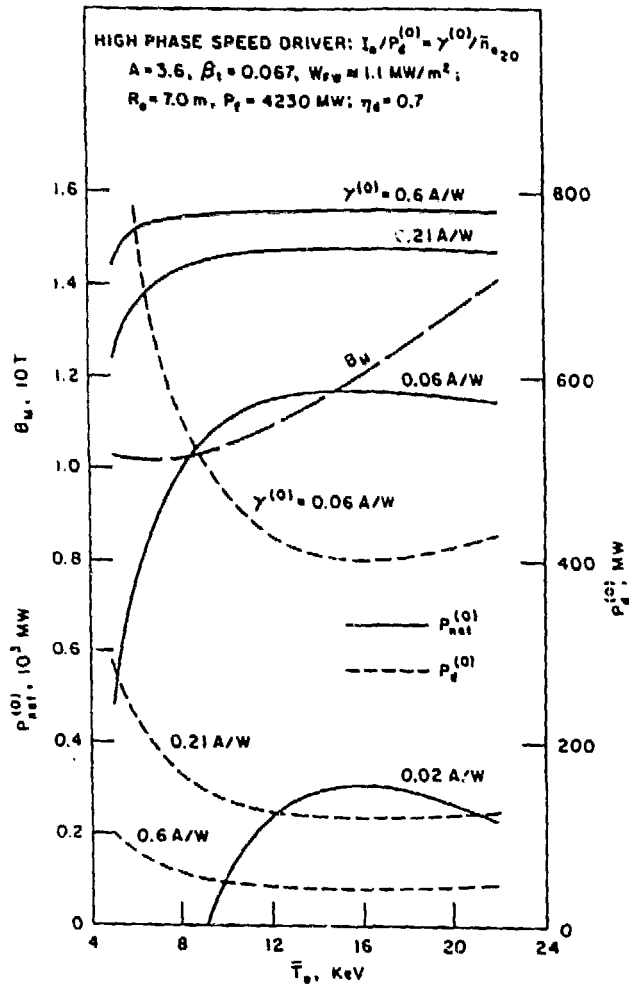


Figure 1. High-speed current drive for various $\gamma^{(0)}$; required driver power, $P_d^{(0)}$, net electric output, $P_{net}^{(0)}$, and magnetic field at the field coil, B_H , for $R_0 = 7.0 \text{ m}$. Electric-to-current drive efficiency assumed to be $\eta_d = 0.7$; high-speed drivers impart energy to superthermal electrons. In this report current drive efficiency, γ , is normalized to 7-m major radius and $1 \times 10^{20} \text{ m}^{-3}$ density.

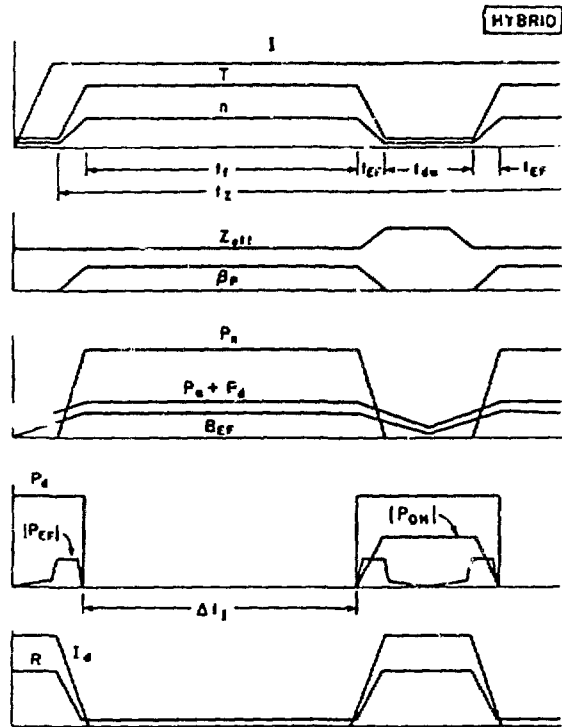


Figure 2. Schematic hybrid burn cycle; plasma resistance, R , and density, n_20 (normalized to $1 \times 10^{20} \text{ m}^{-3}$), are increased and lowered, respectively, to R' and n_20' during the period when the transformer is reset.

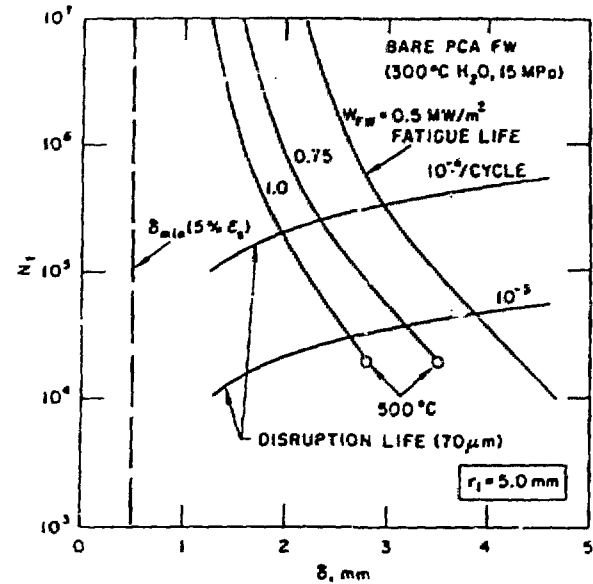


Figure 3. First wall cyclic life versus fatigue and disruption erosion; minimum pipe thickness to withstand rupture, δ_{min} , is set by 5% radiation-induced creep strain.

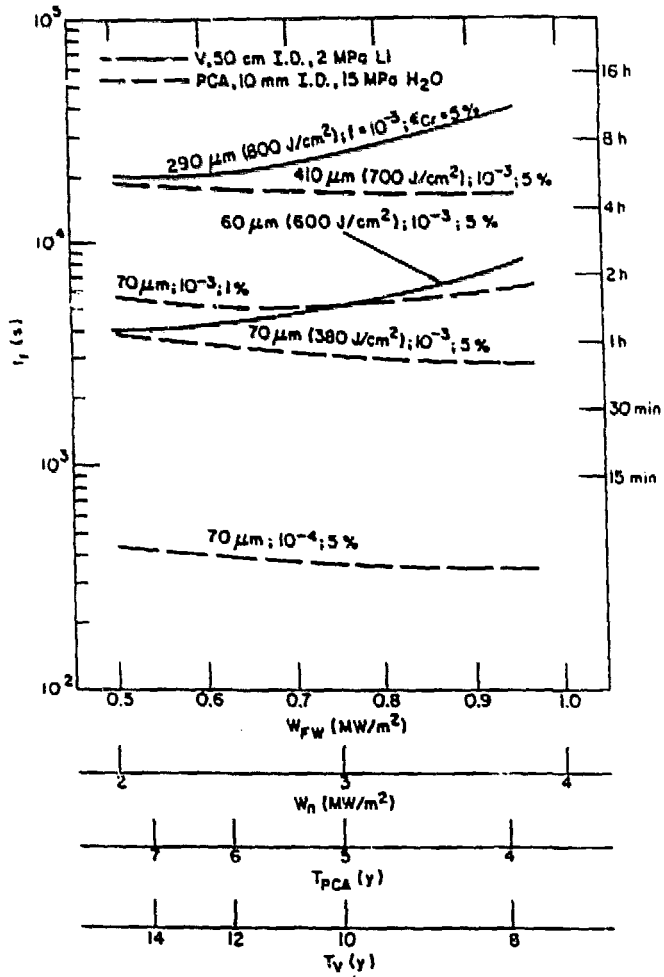


Figure 4. Fusion burn goals to equate cyclic and radiation life of first wall; sputtering is negligible. Component replacement interval is given by lower abscissas.

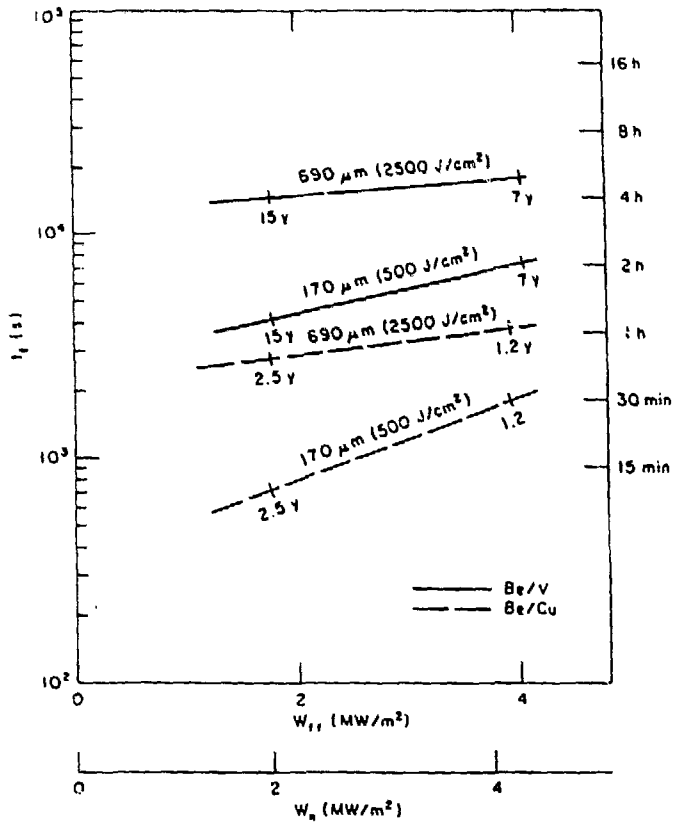


Figure 5. Fusion burn goals to equate cyclic and radiation life of limiter's front face; no sputtering; $f = 10^{-3}$ disruptions/cycle.

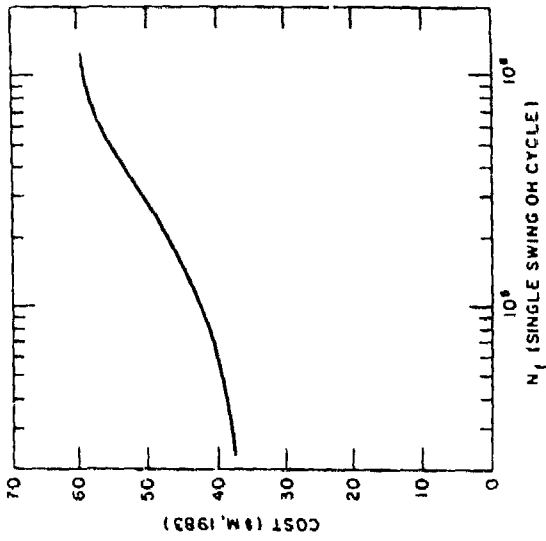


Figure 7. EFC cost vs. number of lifetime fusion burns for DEMO/INTOR.

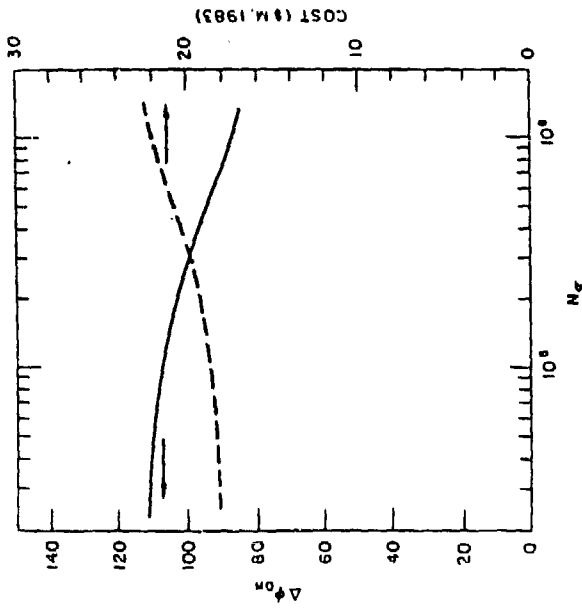


Figure 6. Transformer (OHC) flux, in Webers, and cost vs. the lifetime number of stress cycles for DEMO/INTOR.

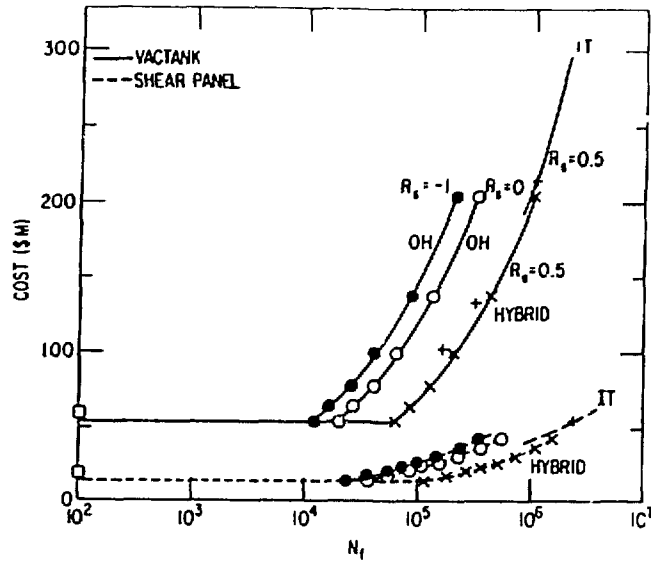


Figure 8. Structure cost for TFC vacuum cases and shear panels. Box indicates CW, 7-m reactor; R_s = minimum stress/maximum stress: 0.5-hybrid, IT; 0 - single swing OH; -1 - double swing OH.

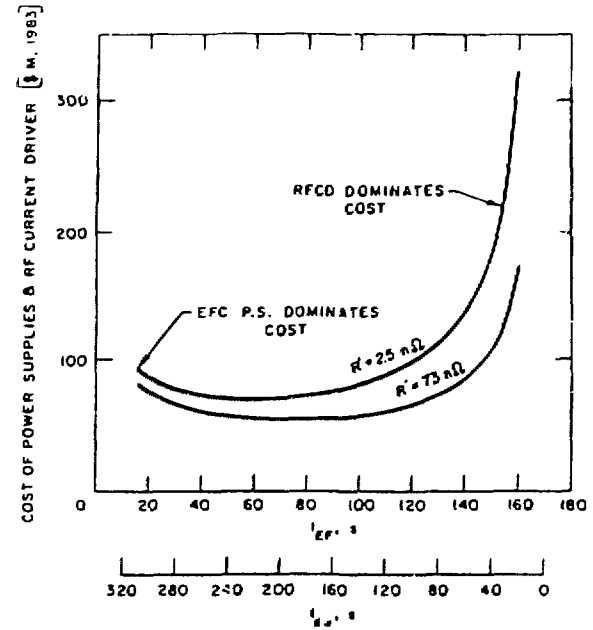


Figure 9. Cost of power supplies and RF current drive system for DEMO/INTOR with hybrid burn cycle with $t_{down} = 340$ s; for resistance during burn $R = R_{sp} = 7.3$ n Ω , $t_f = 1700$ s, so D.F. = 83%; R_{sp} is resistance as OHC is reset; $\gamma/n_2\theta = 1.3$ A/W, \$1.5/W, $\Delta\phi = 108$ V-s.

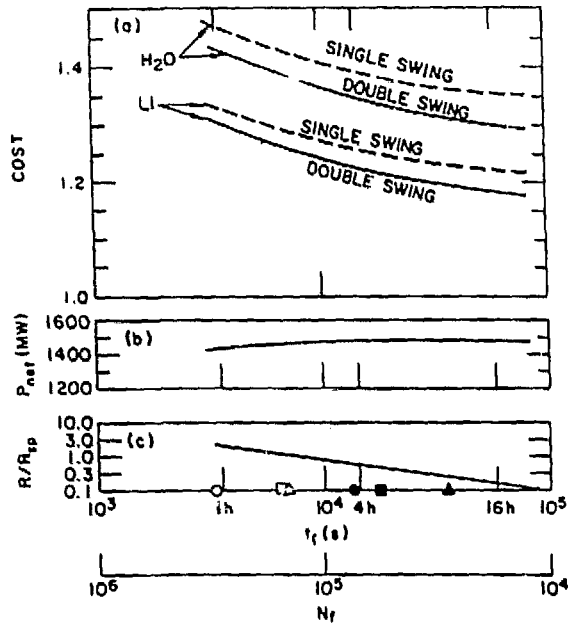


Figure 10. OH cycle; $B_{OH} = 10$ T, 8-m reactor. (a) Upper cost curves represent water thermal storage and near-term magnet costs (C_I), and lower curves represent liquid sodium thermal storage and long-term magnet costs (C_{II}). Cost is total direct capital cost normalized to STARFIRE (Ref. 1) (b) Net electric power. (c) Plasma resistance required to obtain t_f , normalized to Spitzer resistivity, R_{sp} , with $Z_{eff} = 1.70$, $\bar{T}_e = 10$ keV, and $I_0 = 13.0$ MA. Solid symbols are burn goals for worst case disruptions and thermal fatigue; open symbols are goals for moderate disruption damage (circles = limiter's leading edge, squares = limiter's front face, and triangles = first wall).

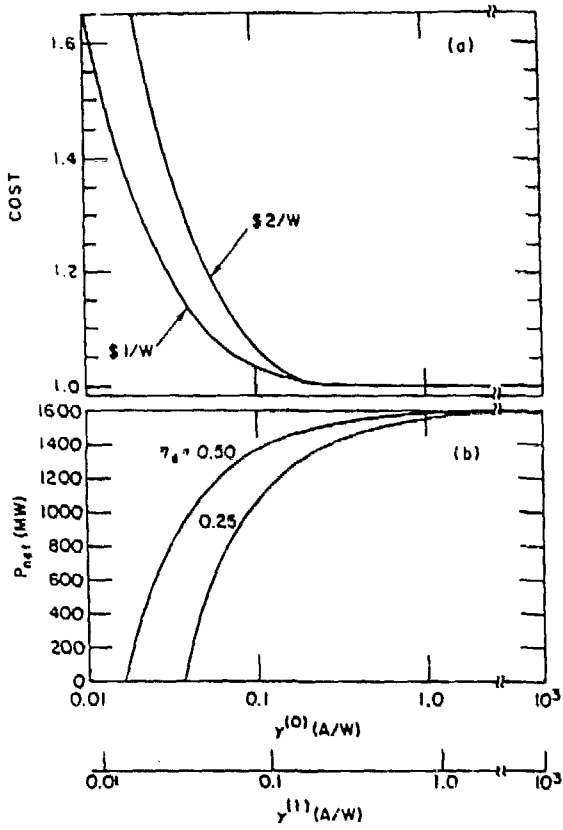


Figure 11. CW cycle; 7-m reactor. (a) Direct capital cost for two values of current drive system cost; EFC winding costed with C_{II} formula. (b) Net power. Upper abscissa applies to high speed current driver, and lower applies to low speed driver. Note: $\bar{T}_e = 12$ keV, $n_{20} = 1.9$, $I_0 = 14.8$ MA.

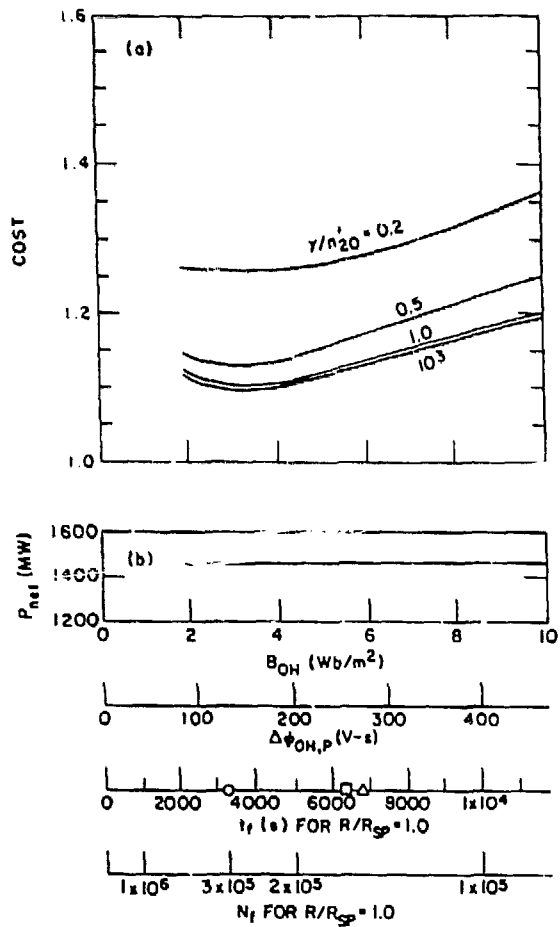


Figure 12. Hybrid cycle; 8-m reactor, $L/R' = 171$ s, driver costed at \$1.5/W. (a) Direct capital cost based on liquid metal thermal storage, long-term magnet costs (C_{LT}), and fatigue assuming $R=R_{sp}$. (b) Net power. Top-most abscissa is full field in the OHC solenoid.